On the Relative Importance of HONO versus HNO_2 in Low-temperature Combustion

Mark E. Fuller[a], C. Franklin Goldsmith[a,*]

[a]*School of Engineering, Brown University, Providence, RI 02912, USA*

Abstract

This work investigates whether both HONO and HNO_2 are essential in describing the reactivity for NO_2-doped ignition experiments or if a strategy could be developed that lumps the two isomers into a single species without adversely affecting the model fidelity. First, the possibility of different product branching fractions is considered; temperature- and pressure-dependent rate constants are computed for H and CH_3 addition to the N=O bond in both HONO and HNO_2. These results suggest that addition of H to HONO and HNO_2 do indeed have different products, but that the results are not likely to have a significant effect. Next, two different approaches to simplifying the HONO submechanism are considered. In the first, HNO_2 is removed from the mechanism. In the second, HNO_2 is replaced with HONO. These two strategies are implemented in different literature mechanisms and then used to compute ignition delay times for H_2 and CH_4. The results show that removing HNO_2 has a modest effect on the ignition delay time, whereas systematically replacing HNO_2 with HONO decreases the predicted ignition delay by approximately a factor of two. The recommendation is that for

*Corresponding author: C. Franklin Goldsmith
Email address: franklin_goldsmith@brown.edu (C. Franklin Goldsmith)

larger fuels, both HONO and HNO_2 should be included in the mechanism.

Keywords: HONO, Nitrogen Chemistry, NOx, Low-temperature Combustion, Chemical Kinetics

1. Introduction

Low-temperature compression ignition (LTCI) engines operate with peak temperatures below 1800 K, avoiding thermal NO_x formation from the nitrogen in the inlet air (NO_x= NO + NO_2)[1, 2]. A critical goal in LTCI engines is understanding the gas-phase chemistry of nitrogen-containing compounds. In experimental studies of LTCI engines with 2-ethylhexyl nitrate (EHN) as the cetane enhancer, only about one-third of the fuel-bound nitrogen is found in the exhaust as NO_x[3, 4, 5]. This result is particularly surprising, since under LTCI engine conditions, it is unclear what the mechanism for NO_x reduction should be. Detailed chemical kinetic models can help to determine the fate of NO_2 below the thermal NO_x limit, provided that the kinetic mechanism includes sufficient fuel-NO_x interactions. However, recent studies strongly suggest that current models do not accurately capture these interactions. For example, a flow reactor study by Giménez-López et al.[6] examined C_2H_4/O_2/NO mixtures under high pressure (60 bar) and temperatures of 600 K to 900 K, and significant removal of NO_x was found experimentally that was not predicted by the kinetic mechanism. A key first step in closing the nitrogen balance for EHN-doped fuels in LTCI engines is understanding how the initial NO_2 that is formed upon dissociation of EHN is further reduced in the cylinder.

NO_2 is unusual in that every atom in the molecule has a radical character, and so both the nitrogen atom and the two oxygen atoms can abstract hydrogen atoms. Accordingly, much of the fuel-bound NO_2 in LTCI engines is converted into one of two isomers, depending upon which atom does the abstraction: nitrous acid (HONO) or nitryl hydride (HNO_2).

The core work on HONO/HNO_2 was compiled and explored by Dean and Bozzelli, as part of their review of gas-phase nitrogen chemistry[7]. More recently, a theoretical analysis of RH + NO_2 for RH = H_2, CH_4, C_2H_6, C_3H_6, C_3H_8, C_4H_8, and C_4H_{10} by Chai and Goldsmith[8] showed that cis-HONO is the dominant product and that trans-HONO, while the most stable isomer, has a production rate approximately an order of magnitude less than cis-HONO. Ongoing work by the authors suggest that cis-HONO and trans-HONO are no longer distinct species under engine relevant conditions, and that they should be treated as a single HONO species in combustion mechanisms.

When NO_2 is involved in an H-transfer reaction – whether H-abstraction from a fuel molecule or disproportionation from a fuel-derived radical – both HONO and HNO_2 are formed. Depending upon the source of the H-atom, the branching fraction for HONO is typically between 60% to 90% of the total flux[8]. HONO and HNO_2 both decompose to the same products: OH + NO (with H + NO_2 also being possible but many orders of magnitude smaller). At high temperatures, this unimolecular decomposition is expected to be faster than any competing bimolecular reaction, but at low temperatures, both HONO and HNO_2 could build up to sufficiently high concentrations that bimolecular reactions are possible[7].

A review of recently published mechanisms reveals inconsistencies with respect to HONO and HNO_2 chemistry. Zhang et al. examined mechanism performance versus experimental data for the combustion of hydrogen and syngas in the presence of NO_x[9]. Drawing on the review in ref. [9], the mechanisms of Abian et al.[10], Ahmed et al.[11], Dagaut et al.[12], Glarborg et al. [6, 13, 14], Konnov[15], and Mathieu et al.[16, 17] are examined. The Dagaut et al. and Konnov mechanisms only considered HONO and omit HNO_2 entirely. The other mechanisms include both species, but typically have 2-3 times the number of HONO reactions as HNO_2. If HONO is formed at a significantly faster rate than HNO_2, and if HNO_2 decomposes at a significantly faster rate than HONO, then the asymmetry of HONO and HNO_2 reactions could be justifiable. If that is the case, however, it also raises the question as to whether HNO_2 contributes anything to the overall kinetics, as implied by the mechanisms of Dagaut et al. and Konnov. A graphical summary of the inclusion of HONO and HNO_2 reactions is presented in Figure 1.

The goal of the present work is to investigate whether or not it is important to maintain HONO and HNO_2 as distinct chemical species in a combustion mechanism. To that end, the manuscript is divided into two sections. The first section addresses the possibility that there could be bimolecular reactions involving HONO and HNO_2 that have different products. One immediate example would be concerted HONO elimination from nitrates and nitrites, since there is no analogous concerted HNO_2 elimination. The reaction family we will focus on is radical addition to a double bond, since in principle radical addition to the N=O bond, followed by isomerization and/or

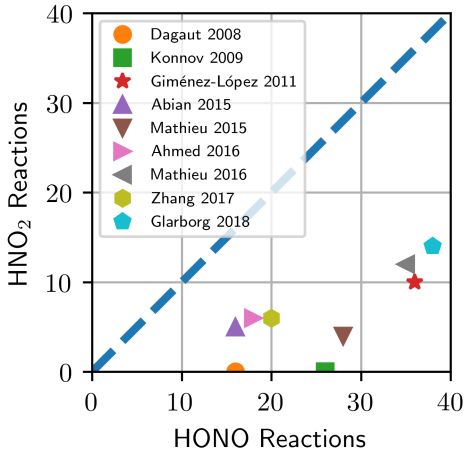

Figure 1: Number of HONO and HNO_2 reactions included in recent mechanisms.

beta-scission, could yield different products for HONO and HNO_2. If radical addition to HONO and HNO_2 is going to compete with unimolecular decomposition reactions, then the radical must be present in high concentrations. Accordingly, we focus on H and CH_3, as these two radicals are ubiquitous in combustion and have comparatively high concentrations for a radical.

Limited experimental data are available for the elementary reactions of interest. Slack and Grillo published an estimate for the rate H_2 + NO_2 proceeding to H + HNO_2 in 1978[18]. Later work by Park et al.[19] offered a lower rate for this reaction, which was employed by Mueller et al.[20] in modeling of a turbulent flow reaction. Subsequent work by Mueller at al.[21] directly addressed this rate constant, offering a new fit based on experimental data. This revision was in good agreement with the result of Park et al. The reliability of the data and rate constants offered by Slack and Grillo was called into question by Mueller et al. based upon a discussion of the details

of the original experiments. For all of these experiments, it appears that no distinction between HONO and HNO_2 was made and that they were treated as a single species. In no case was the rate of the elementary reaction to H and HONO directly observed. For the reaction of CH_4 and NO_2 to form CH_3 and HONO, there appears only to be a study conducted by Slack and Grillo[22]. A comparison between the present work and the prior experimental data is provided in the Supplemental Material.

The second section quantifies the extent to which inclusion of HNO_2 in a mechanism is superfluous to combustion kinetics. Two literature mechanisms were adapted: Mathieu et al. [17] and Glarborg et al.[14]. These two mechanisms were selected because they come from independent research groups and have been validated against a broad range of experimental targets. For each mechanism, four sets of ignition-delay calculations were performed. First, the published mechanism was used without modification. Second, the HONO/HNO_2 reactions in the original mechanism are replaced by a newly developed, theory-derived HONO/HNO_2 submechanism. The thermodynamic properties for the species in the new HONO submechanism are taken from the Active Thermochemical Tables, version v1.122b[23, 14]. The third and fourth modifications address the question of lumping HONO and HNO_2. In one case, all reactions involving HNO_2 are simply removed from the mechanism ("No HNO_2" below). This approach to lumping is expected to underpredict the flux through RH + NO_2 $\rightleftharpoons$ R + HONO and thus decrease the overall reactivity. As a counter to this effect, the latter approach to lumping systematically replaces 'HNO2' with 'HONO' in the mechanism file, and the new HONO reactions are treated as duplicates ("Duplicate"

below) This process is repeated for both H_2 and CH_4 ignition delays.

2. Computational Methods

As mentioned above, the work of Chai and Goldsmith treated cis- and trans-HONO separately, whereas our current model assumes that these two conformers should be lumped into a single species. Accordingly, the transition state theory (TST) calculations for the direct H-abstraction that were performed in Ref. 8 were redone with a single HONO isomer that systematically treats the cis- trans- conversion as a hindered internal rotation in both the reactant and transition state. These calculations used the ANL0 compound method for both the energetics and the structures and frequencies[24]. Additionally, these results are now presented in the exothermic direction (*e.g.* $R + HONO/HNO_2 \rightleftharpoons RH + NO_2$). For the new addition/isomerization/elimination pathways in the present work, the compound method recommended by Chai and Goldsmith was used[8]. Geometry optimization and normal mode analysis were performed using the B2PLYPD3 functional with the cc-pVTZ basis set[25, 26, 27]. Single-point calculations were performed on the optimized geometries at the UCCSD(T)-F12a/cc-pVTZ-f12 level[28, 29, 30]. For transition states that have a first-order saddle point in potential energy, standard rigid-rotor harmonic-oscillator models were used to compute the microcanonical rate coefficients; torsional modes were treated separately, with rotational scans performed in 10° increments, and the partition function was computed via summation over the energy levels for the corresponding 1D Schrödinger equation. The two transition states that lead to OH formation, $HONHO \rightarrow HNO + OH$ and $CH_3N(O)OH \rightarrow CH_3NO + OH$, had compara-

tively wide saddle points that exhibited strong multireference effects. These two transition states were treated using CASPT2(5e4o)/cc-pVTZ, where the active space consisted of the (π, π^*) orbitals in RNO, plus the radical orbital and lone pair in OH, averaged over two states to account for the spatial degeneracy in OH. All DFT calculations were performed using Gaussian09[31]; all wavefunction calculations were performed using MOLPRO[32].

Transition state theory (TST) calculations were performed using the RRKM/ME code MESS[33, 34], which is part of the computational kinetics package PAPR developed by Argonne National Laboratory[35]. A single exponential was used to model the collisional energy transfer, with $\langle \Delta E_{\text{down}} \rangle = 200\,(T/298[\text{K}])^{0.85}$ cm^{-1}. The resulting phenomenological rate constants we converted into the PLOG formalism and formatted for use in CANTERA[36]. All kinetic simulations were performed using CANTERA. The ignition delay time was defined as the time at which the simulated concentration of OH was maximum.

3. Results

3.1. Computational Kinetics

3.1.1. H + HONO/HNO_2

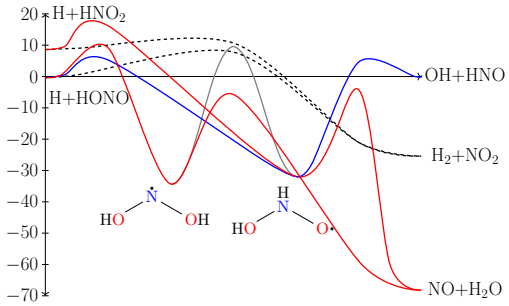

Figure 2: PES for H + HONO and H + HNO_2, relative to H + HONO. The solid lines correspond to addition/isomerization/elimination. The dashed lines are the competing direct abstraction pathways. Energies are in kcal/mole.

The stationary points for the potential energy surface (PES) for the addition of H to HONO and HNO_2 are shown in Figure 2. For H + HONO, the barrier height for addition to the nitrogen is lower than the competing direct abstraction by 1.2 kcal/mole; consequently, the dominant product channel for H + HONO is NO + H_2O, with H_2 + NO_2 being a close second, followed by OH + HNO. For H + HNO_2, in contrast, the barrier height for addition to the oxygen is higher than the competing direct abstraction by 5.6 kcal/mole, and so direct abstraction is the dominant pathway for all conditions. Neither system exhibits much pressure dependence (not shown). The results for H + HONO/HNO_2 are summarized for 1 atm in Table 1. The corresponding branching fractions are shown in Figure 3a for H + HONO and Figure 3b for H + HNO_2.

Table 1: Computed constants for reactions at 1 atm for H + $HONO/HNO_2$. Pathways are addition/isomerization/elimination reactions unless otherwise noted. Rate constants are of the form $k(T) = A(T/T_0^n)exp[-E_a/RT]$ with A in $cm^3mol^{-1}s^{-1}$, T_0=1 K, E_a in kcal $mole^{-1}$.

Reaction	A	n	E_a	k(1000 K)
H + HONO = H_2 + NO_2 [a]	1.9×10^3	2.8	1.4	2.9×10^{11}
H + HNO_2 = H_2 + NO_2 [a]	2.3×10^4	2.8	-2.0	1.3×10^{13}
H + HNO_2 = NO + H_2O	3.4×10^9	1.1	5.6	3.3×10^{11}
H + HNO_2 = OH + HNO	3.7×10^7	1.8	5.6	4.8×10^{11}
H + HONO = NO + H_2O	4.3×10^9	1.0	4.1	4.8×10^{11}
OH + HNO = H + HONO	1.5×10^3	2.7	4.6	2.2×10^{10}

[a] Abstraction

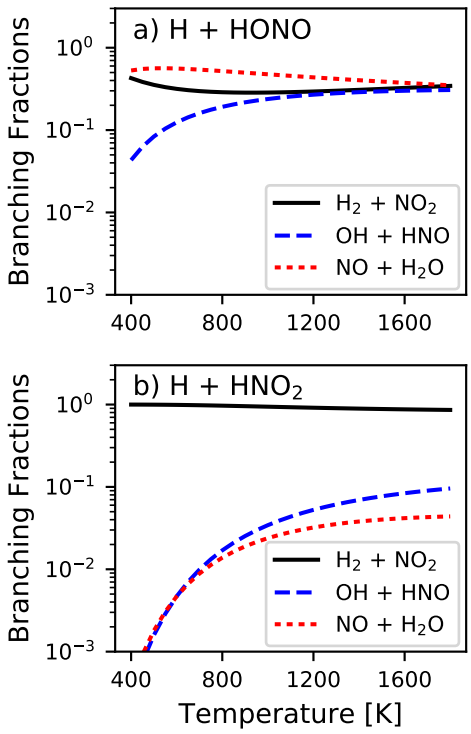

Figure 3: a) branching fractions at 1 atm for H + HONO. b) branching fractions at 1 atm for H + HNO_2. The branching fraction includes the contribution of both the addition/isomerization/elimination pathways and the direct abstraction pathway (dashed and solid lines in Figure 2, respectively).

3.1.2. CH_3 + HONO/HNO_2

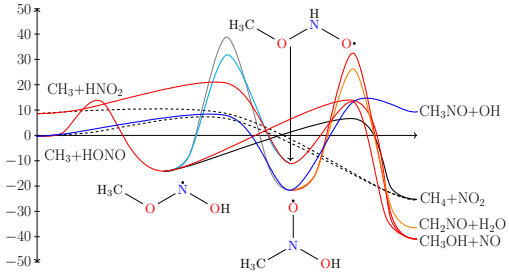

Figure 4: PES for CH_3 + HONO and CH_3 + HNO_2, relative to CH_3 + HONO. The solid lines correspond to addition/isomerization/elimination. The dashed lines are the competing direct abstraction pathways. Energies are in kcal/mole.

The PES for the addition of CH_3 to HONO and HNO_2 is shown in Figure 4. Unlike the case for H + HONO, the barrier height for direct abstraction is 2.2 kcal/mol lower in energy than addition to either the O or N atom. Consequently, direct abstraction dominates for both HONO and HNO_2 for all temperatures and pressures. The results for CH_3 + HONO/HNO_2 are summarized for 1 atm in Table 2. The corresponding branching fractions are shown in Figure 5a for CH_3 + HONO and Figure 5b for CH_3 + HNO_2.

Table 2: Computed constants at 1 atm for CH_3 + $HONO/HNO_2$. Pathways are addition/isomerization/elimination reactions unless otherwise noted. Rate constants are of the form $k(T) = A(T/T_0^n)exp[-E_a/RT]$ with A in $cm^3mol^{-1}s^{-1}$, T_0=1 K, E_a in kcal $mole^{-1}$.

Reaction	A	n	E_a	k(1000 K)
CH_3 + HONO = CH_4 + NO_2[a]	3.6×10^{-4}	4.4	-0.4	7.6×10^{9}
CH_3 + HNO_2 = CH_4 + NO_2[a]	2.2×10^{3}	2.8	-2.9	1.9×10^{12}
CH_3 + HNO_2 = CH_4 + NO_2	6.6×10^{-3}	4.1	18.4	9.7×10^{5}
CH_3 + HNO_2 = CH_3OH + NO	4.7×10^{11}	0.2	13.6	1.6×10^{9}
CH_3 + HNO_2 = CH_2NO + H_2O	5.9×10^{-25}	9.1	27.2	1.3×10^{-3}
CH_3 + HONO = CH_4 + NO_2	3.2×10^{4}	2.1	11.9	2.1×10^{8}
CH_3 + HONO = CH_3OH + NO	6.4×10^{-2}	3.3	12.7	9.0×10^{5}
CH_3 + HONO = CH_2NO + H_2O	3.3×10^{-2}	3.5	20.7	2.3×10^{4}
CH_3NO + OH = CH_3 + HONO	1.5×10^{9}	1.0	4.6	1.1×10^{11}

[a] Abstraction

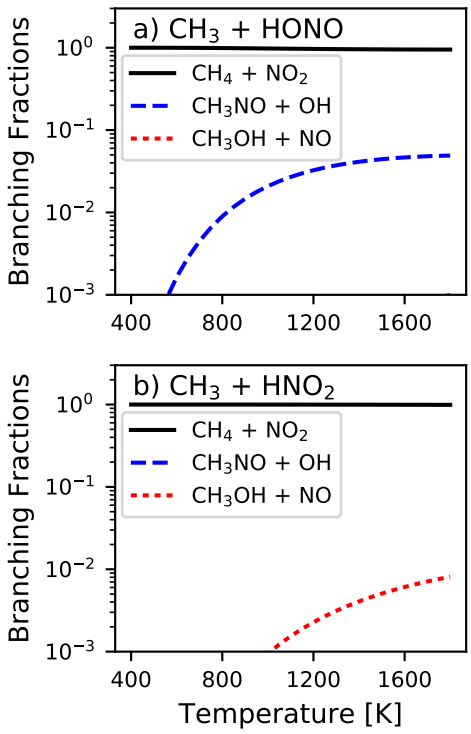

Figure 5: a) branching fractions at 1 atm for CH_3 + HONO. b) branching fractions at 1 atm for CH_3 + HNO_2. The branching fraction includes the contribution of both the addition/isomerization/elimination pathways and the direct abstraction pathway (dashed and solid lines in Figure 4, respectively).

3.2. Ignition Delay Simulations

For the H_2 ignition delays, the initial composition was 1.0% H_2, 1.0% O_2, 0.16% NO_2, and the remainder Ar at 1.56 atm, as described in ref. [9]; these results are presented in Figures 6 and 7 for the modifications to the Mathieu et al. and Glarborg et al. mechanisms, respectively. The original mechanism (solid black) and the same mechanism with the substituted HONO/HNO_2 submechanism (dashed blue) are in close agreement for both the Mathieu et

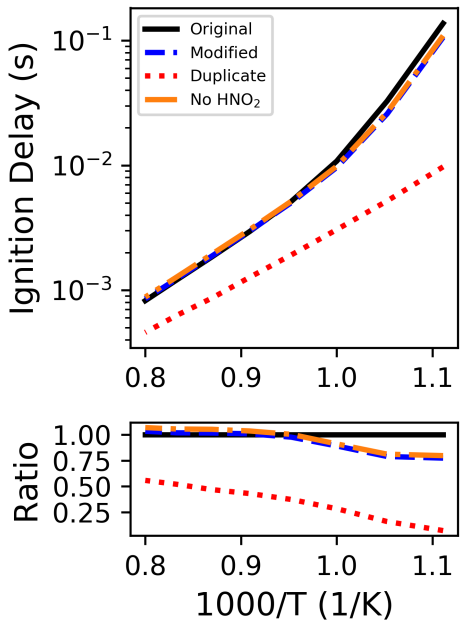

Figure 6: Ignition delay for H_2, $\phi = 0.5$ doped with 1600 ppm NO_2 at 1.56 atm, Mathieu et al. mechanism

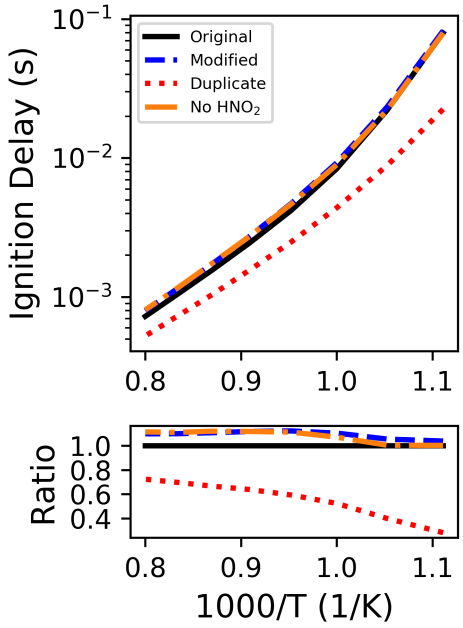

Figure 7: Ignition delay for H_2, $\phi = 0.5$ doped with 1600 ppm NO_2 at 1.56 atm, Glarborg et al. mechanism

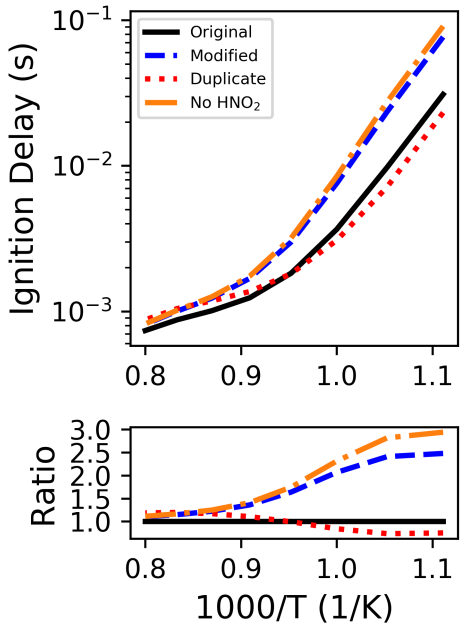

Figure 8: Ignition delay for CH_4, $\phi = 1.0$ doped with 0.15% NO_2 at 9 atm, Mathieu et al. mechanism

al. and Glarborg et al. mechanisms. Additionally, simply removing HNO_2 from the mechanism (dash-dot orange) has little effect. Replacing 'HNO2' with 'HONO' (dotted red), in contrast, has a substantial effect on the ignition delay, effectively decreasing τ by more than a factor of two. The cause of this effect will be discussed below in Section 4.

For the CH_4 ignition delays, the initial composition was 9.49% CH_4, 19.0% O_2, 56.7% N_2, 14.6% Ar, and 0.15% NO_2 at 9 atm, as described in ref. [16]; these results are presented in Figures 8 and 9 for the modifications to the Mathieu et al. and Glarborg et al. mechanisms, respectively. Whereas the modifications to the two mechanisms were both qualitatively and quantitatively similar for H_2 ignition, the changes to the mechanisms for CH_4

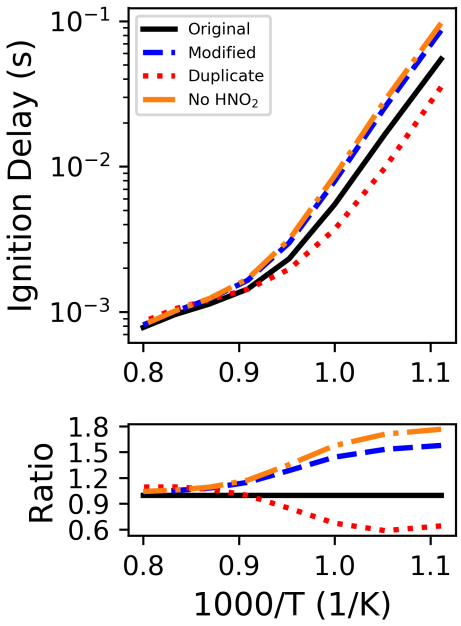

Figure 9: Ignition delay for CH_4, $\phi = 1.0$ doped with 0.15% NO_2 at 9 atm, Glarborg et al. mechanism

ignition yield different, slightly more pronounced trends. The changes to the Glarborg mechanism, Figure 9, are qualitatively similar to Figure 7, with the new submechanism having a retarding effect, and the "Duplicate" strategy of combining HNO_2 with HONO decreases the ignition delay by nearly a factor of two at the lowest temperatures. The changes to the Mathieu mechanism, Figure 8, in contrast, show a much smaller response to the 'Duplicate" strategy, but the ignition delay time increases by an even greater factor than the Glarborg et al. mechanism when the new submechanism is used. In both cases, the ignition delay time is sensitive to the HONO/HNO_2 submechanism for $T < 1400$ K. At higher temperatures, the contribution of NO_2 decreases, and the conventional high-temperature oxidation chemistry begins to dominate.

4. Discussion

Although the results for H + HONO/HNO_2 shown in Figure 3 confirm that it is possible for R + HONO/HNO_2 to yield different products, it is unlikely that this effect will be significant. For H + HONO, the largest rate constant is for the OH + HNO product channel; assuming that HNO rapidly dissociates to H + NO, this reaction is effectively little more than H-catalyzed HONO decomposition. Our expectation is the CH_3 + HONO/HNO_2 is more typical of other radicals in that direct abstraction will always be favored over addition/isomerization/elimination, and therefore it is unlikely that bimolecular reactions involving R + HONO/HNO_2 will have product branching fractions that are significantly different. Finally, the "Direct Hydrogen Transfer" approach of Dean and Bozzelli [7] works reasonably well for R + HONO but

appears to systematically underestimate the rate constants for R + HNO_2.

When HNO_2 is omitted from the substituted mechanism entirely (dash-dot orange), the predicted ignition delay time increases slightly, but the magnitude of the effect is negligible for H_2 and CH_4. By removing HNO_2, the net flux of H_2 + NO_2 is decreased slightly, which leads to a slight decrease in the net rate of chain branching through the subsequent decomposition of HNO_2. However, when HNO_2 is replaced with HONO and added to the total rate, the effect is far more pronounced. This effect is due to the fact that the reactions H + HONO $\rightleftharpoons$ H_2 + NO_2 and H + HNO_2 $\rightleftharpoons$ H_2 + NO_2 are running in the "reverse" (endothermic) direction. In the forward direction, the rate constant for H + HNO_2 is larger than that for H + HONO by nearly an order of magnitude, owing to the fact that the former is more exothermic. In the reverse direction, the rate constant for the formation of H + HNO_2 is smaller by nearly an order of magnitude. If the larger forward rate for H + HNO_2 is added to H + HONO, but the reverse rate constant is computed using the thermodynamic properties for HONO (as is happening in the "duplicate" approach), then the net rate constant for H_2 + NO_2 $\rightarrow$ H + HONO is now over-predicted by a factor of 50. Since the subsequent decomposition of HONO makes this reaction net chain branching, over-predicting the flux through H_2 + NO_2 significantly increases the reactivity of the mixture.

The same effect can be seen for the CH_4 ignition delays. Removing HNO_2 entirely slightly reduces the reactivity, whereas replacing HNO_2 with HONO dramatically accelerates ignition. The one qualitative difference is that the new HONO/HNO_2 mechanism appears to have a larger effect when substituted into the mechanism of Mathieu et al. than Glarborg et al. These two

mechanisms use different rate constants for both CH_3 + HONO $\rightleftharpoons$ CH_4 + NO_2 and CH_3 + HNO_2 $\rightleftharpoons$ CH_4 + NO_2. Glarborg et al. obtains both from the work of Chai and Goldsmith[8]. Mathieu et al. obtains the rate constant for CH_3 + HONO $\rightleftharpoons$ CH_4 + NO_2 from Dean and Bozzelli [7]. This value is approximately a factor of two greater than that in the present work. Mathieu et al. takes their values for CH_3 + HNO_2 $\rightleftharpoons$ CH_4 + NO_2 from Yamaguchi et al.[37]. The rate constant from Yamaguchi et al. for CH_3 + HNO_2 $\rightleftharpoons$ CH_4 + NO_2 is greater than that of the present work by about a factor of five. Consequently, the flux through CH_4 + NO_2 $\rightleftharpoons$ CH_3 + HNO_2 is much larger in the original Mathieu et al. mechanism, and since HNO_2 has a larger rate constant for thermal decomposition, this higher flux effectively leads to faster chain branching through HNO_2.

In summary, the somewhat naive approach of "lumping" together HNO_2 and HONO is not a successful strategy because it will over-estimate net flux of RH + NO_2 and thence chain branching. The alternative approach of simply omitting HNO_2 altogether has a much smaller effect. However, the fact that the effect is so small for the present case of H_2 and CH_4 is likely an outlier. As discussed in ref. [8], the branching fraction for RH + NO_2 $\rightleftharpoons$ R + HNO_2 increases with the size of RH, from $\sim$10% for H_2 and CH_4, to $\sim$40% for C_4H_8 and C_4H_{10}. For this reason, it will be preferable to include HNO_2 for larger mechanisms, but these reactions should be included systematically, with rate coefficients for both HONO and HNO_2.

5. Conclusion

The kinetic implications of HONO versus HNO_2 are presented. New rate constants are computed for the addition of H and CH_3 to the double bonds in HONO and HNO_2. These results confirm that bimolecular reactions involving HONO/HNO_2 could have different products. Modeling studies, however, suggest that this result is unlikely to have a significant effect. Two approaches at removing HNO_2 were considered. In the first approach, HNO_2 is simply deleted from the mechanism. This approach has a modest effect on ignition delay times for H_2 and CH_4, but it is expected to underpredict the reactivity significantly for larger hydrocarbons. The second approach replaces HNO_2 with HONO. This approach dramatically increases the reactivity of the mixture by over-estimating the net contribution of RH + NO_2.

Acknowledgments

This work is supported by the U.S. National Science Foundation through Award Number CBET-1553366, with Dr. Song-Charng Kong as the program manager. MEF gratefully acknowledges help from Aaron Danilack and Xi Chen with the electronic structure theory calculations.

Supplementary Materials

The cartesian coordinates and vibrational frequencies for the $H_2N_1O_2$ and $H_4C_1N_1O_2$ PES calculations are provided, as are the temperature and pressure dependent rate coefficients. A comparison of the rate constants used in modeling to experimental data is also provided as a supplement.

References

[1] R. D. Reitz, G. Duraisamy, Review of high efficiency and clean reactivity controlled compression ignition (RCCI) combustion in internal combustion engines, Prog. Energy Combust. Sci. 46 (2015) 12–71.

[2] A. K. Agarwal, A. P. Singh, R. K. Maurya, Evolution, challenges and path forward for low temperature combustion engines, Prog. Energy Combust. Sci. 61 (2017) 1 – 56.

[3] A. B. Dempsey, N. R. Walker, R. D. Reitz, Effect of cetane improvers on gasoline, ethanol, and methanol reactivity and the implications for RCCI combustion, SAE International Journal of Fuels and Lubricants 6 (1) (2013) 170–187.

[4] D. A. Splitter, R. D. Reitz, Fuel reactivity effects on the efficiency and operational window of dual-fuel compression ignition engines, Fuel 118 (2014) 163–175.

[5] A. M. Ickes, S. V. Bohac, D. N. Assanis, Effect of 2-ethylhexyl nitrate cetane improver on NO_x emissions from premixed low-temperature diesel combustion, Energy & Fuels 23 (10) (2009) 4943–4948.

[6] J. Giménez-López, M. Alzueta, C. Rasmussen, P. Marshall, P. Glarborg, High pressure oxidation of C_2H_4/NO mixtures, Proc. Comb. Inst. 33 (1) (2011) 449–457.

[7] A. M. Dean, J. W. Bozzelli, Combustion Chemistry of Nitrogen, Springer New York, New York, NY, 2000, Ch. 2, pp. 125–341.

[8] J. Chai, C. F. Goldsmith, Rate coefficients for fuel + NO_2 : Predictive kinetics for HONO and HNO_2 formation, Proc. Comb. Inst. 36 (1) (2017) 617–626.

[9] Y. Zhang, O. Mathieu, E. L. Petersen, G. Bourque, H. J. Curran, Assessing the predictions of a NO_x kinetic mechanism on recent hydrogen and syngas experimental data, Combust. Flame 182 (2017) 122–141.

[10] M. Abian, M. U. Alzueta, P. Glarborg, Formation of NO from N_2/O_2 mixtures in a flow reactor: Toward an accurate prediction of thermal NO, Int. J. Chem. Kinet. 47 (8) (2015) 518–532.

[11] S. F. Ahmed, J. Santner, F. L. Dryer, B. Padak, T. I. Farouk, Computational study of NO_x formation at conditions relevant to gas turbine operation, part 2: NO_x in high hydrogen content fuel combustion at elevated pressure, Energy & Fuels 30 (9) (2016) 7691–7703.

[12] P. Dagaut, P. Glarborg, M. Alzueta, The oxidation of hydrogen cyanide and related chemistry, Prog. Energy Combust. Sci. 34 (1) (2008) 1–46.

[13] J. Gimenez-Lopez, C. T. Rasmussen, H. Hashemi, M. U. Alzueta, Y. Gao, P. Marshall, C. F. Goldsmith, P. Glarborg, Experimental and kinetic modeling study of C_2H_2 oxidation at high pressure, Int. J. Chem. Kinet. 48 (11) (2016) 724–738.

[14] P. Glarborg, J. A. Miller, B. Ruscic, S. J. Klippenstein, Modeling nitrogen chemistry in combustion, Prog. Energy Combust. Sci. 67 (2018) 31–68.

[15] A. Konnov, Implementation of the NCN pathway of prompt-NO formation in the detailed reaction mechanism, Combust. Flame 156 (11) (2009) 2093–2105.

[16] O. Mathieu, J. M. Pemelton, G. Bourque, E. L. Petersen, Shock-induced ignition of methane sensitized by NO_2 and N_2O, Combust. Flame 162 (8) (2015) 3053–3070.

[17] O. Mathieu, B. Giri, A. Agard, T. Adams, J. Mertens, E. Petersen, Nitromethane ignition behind reflected shock waves: Experimental and numerical study, Fuel 182 (2016) 597–612.

[18] M. Slack, A. Grillo, Rate coefficients for $H_2 + NO_2 = HNO_2 + H$ derived from shock tube investigations of $H_2/O_2/NO_2$ ignition, Combustion and Flame 31 (1978) 275–283.

[19] J. Park, N. D. Giles, J. Moore, M. C. Lin, A comprehensive kinetic study of thermal reduction of NO_2 by H_2, The Journal of Physical Chemistry A 102 (49) (1998) 10099–10105.

[20] M. A. Mueller, R. A. Yetter, F. L. Dryer, Kinetic modeling of the $CO/H_2O/O_2/NO/SO_2$ system: Implications for high-pressure fall-off in the $SO_2 + O(+M) = SO_3(+M)$ reaction, Int. J. Chem. Kinet. 32 (6) (2000) 317–339.

[21] M. A. Mueller, J. L. Gatto, R. A. Yetter, F. L. Dryer, Hydrogen/nitrogen dioxide kinetics: derived rate data for the reaction $H_2 + NO_2 = HONO + H$ at 833 K, Combustion and Flame 120 (4) (2000) 589–594.

[22] M. Slack, A. Grillo, Shock tube investigation of methane-oxygen ignition sensitized by NO_2, Combustion and Flame 40 (1981) 155–172.

[23] B. Ruscic, D. H. Bross, Active thermochemical tables (ATcT) values based on ver. 1.122 of the thermochemical network., `https://atct.anl.gov/`.

[24] S. J. Klippenstein, L. B. Harding, B. Ruscic, Ab initio computations and active thermochemical tables hand in hand: Heats of formation of core combustion species, J. Phys. Chem. A 121 (2017) 6580–6602.

[25] S. Grimme, Semiempirical hybrid density functional with perturbative second-order correlation, J. Chem. Phys. 124 (3) (2006) 034108.

[26] S. Grimme, J. Antony, S. Ehrlich, H. Krieg, A consistent and accurate ab initio parametrization of density functional dispersion correction (DFT-D) for the 94 elements H-Pu, J. Chem. Phys. 132 (15) (2010) 154104.

[27] L. Goerigk, S. Grimme, A thorough benchmark of density functional methods for general main group thermochemistry, kinetics, and noncovalent interactions, Phys. Chem. Chem. Phys. 13 (14) (2011) 6670.

[28] T. B. Adler, G. Knizia, H.-J. Werner, A simple and efficient CCSD(t)-F12 approximation, J. Chem. Phys. 127 (22) (2007) 221106.

[29] T. B. Adler, H.-J. Werner, F. R. Manby, Local explicitly correlated second-order perturbation theory for the accurate treatment of large molecules, J. Chem. Phys. 130 (5) (2009) 054106.

[30] G. Knizia, T. B. Adler, H.-J. Werner, Simplified CCSD(t)-F12 methods: Theory and benchmarks, J. Chem. Phys. 130 (5) (2009) 054104.

[31] M. J. Frisch, G. W. Trucks, H. B. Schlegel, G. E. Scuseria, M. A. Robb, J. R. Cheeseman, G. Scalmani, V. Barone, G. A. Petersson, H. Nakatsuji, X. Li, M. Caricato, A. V. Marenich, J. Bloino, B. G. Janesko, R. Gomperts, B. Mennucci, H. P. Hratchian, J. V. Ortiz, A. F. Izmaylov, J. L. Sonnenberg, D. Williams-Young, F. Ding, F. Lipparini, F. Egidi, J. Goings, B. Peng, A. Petrone, T. Henderson, D. Ranasinghe, V. G. Zakrzewski, J. Gao, N. Rega, G. Zheng, W. Liang, M. Hada, M. Ehara, K. Toyota, R. Fukuda, J. Hasegawa, M. Ishida, T. Nakajima, Y. Honda, O. Kitao, H. Nakai, T. Vreven, K. Throssell, J. A. Montgomery, Jr., J. E. Peralta, F. Ogliaro, M. J. Bearpark, J. J. Heyd, E. N. Brothers, K. N. Kudin, V. N. Staroverov, T. A. Keith, R. Kobayashi, J. Normand, K. Raghavachari, A. P. Rendell, J. C. Burant, S. S. Iyengar, J. Tomasi, M. Cossi, J. M. Millam, M. Klene, C. Adamo, R. Cammi, J. W. Ochterski, R. L. Martin, K. Morokuma, O. Farkas, J. B. Foresman, D. J. Fox, Gaussian09 Revision D.01, gaussian Inc. Wallingford CT (2013).

[32] H.-J. Werner, P. J. Knowles, G. Knizia, F. R. Manby, M. Schütz, P. Celani, W. Györffy, D. Kats, T. Korona, R. Lindh, A. Mitrushenkov, G. Rauhut, K. R. Shamasundar, T. B. Adler, R. D. Amos, A. Bernhardsson, A. Berning, D. L. Cooper, M. J. O. Deegan, A. J. Dobbyn, F. Eckert, E. Goll, C. Hampel, A. Hesselmann, G. Hetzer, T. Hrenar, G. Jansen, C. Köppl, Y. Liu, A. W. Lloyd, R. A. Mata, A. J. May, S. J. McNicholas, W. Meyer, M. E. Mura, A. Nicklass,

D. P. O'Neill, P. Palmieri, D. Peng, K. Pflüger, R. Pitzer, M. Reiher, T. Shiozaki, H. Stoll, A. J. Stone, R. Tarroni, T. Thorsteinsson, M. Wang, Molpro, version 2015.1, a package of ab initio programs, see http://www.molpro.net (2015).

[33] Y. Georgievskii, J. A. Miller, M. P. Burke, S. J. Klippenstein, Reformulation and solution of the master equation for multiple-well chemical reactions, J. Phys. Chem. A 117 (2013) 12146–12154.

[34] Y. Georgievskii, S. J. Klippenstein, MESS: Master equation system solver 2016.3.23, `http://tcg.cse.anl.gov/papr/codes/mess.html/`.

[35] Y. Georgievskii, J. A. Miller, M. P. Burke, S. J. Klippenstein, PAPR: Predictive automated phenomenological rates v1, `http://tcg.cse.anl.gov/papr/`.

[36] D. G. Goodwin, H. K. Moffat, R. L. Speth, Cantera: An object-oriented software toolkit for chemical kinetics, thermodynamics, and transport processes, `http://www.cantera.org`, version 2.2.1 (2016).

[37] Y. Yamaguchi, Y. Teng, S. Shimomura, K. Tabata, K. Suzuki, Ab initio study for selective oxidation of methane with NO_x (x= 1, 2), J. Phys. Chem. A 103 (1999) 8272–8278.